LRRTM3 promotes processing of amyloid-precursor protein by BACE1 and is a positional candidate gene for late-onset Alzheimer's disease

John Majercak*, William J. Ray*, Amy Espeseth†, Adam Simon*, Xiao-Ping Shi*, Carrie Wolffe*, Krista Getty*, Shane Marine‡, Erica Stec‡, Marc Ferrer‡, Berta Strulovici‡, Steven Bartz§, Adam Gates†, Min Xu†, Qian Huang†, Lei Ma*, Paul Shughrue*, Julja Burchard§, Dennis Colussi*, Beth Pietrak*, Jason Kahana*, Dirk Beher¶, Thomas Rosahl¶, Mark Shearman¶, Daria Hazuda†, Alan B. Sachs‖, Kenneth S. Koblan*, Guy R. Seabrook*, and David J. Stone‖**

Department of *Alzheimer's Research, †Molecular and Cellular Technology, and ‡Automated Biotechnology, Merck & Co., Inc., West Point, PA 19486; Departments of §Biology and ‖Molecular Profiling, Rosetta Inpharmatics LLC, Seattle, WA 98109; and ¶Department of Alzheimer's Research, Merck Research Laboratories, Boston, MA 02115

Edited by L. L. Iversen, University of Oxford, Oxford, United Kingdom, and approved September 27, 2006 (received for review June 30, 2006)

Rare familial forms of Alzheimer's disease (AD) are thought to be caused by elevated proteolytic production of the Aβ42 peptide from the β-amyloid-precursor protein (APP). Although the pathogenesis of the more common late-onset AD (LOAD) is not understood, BACE1, the protease that cleaves APP to generate the N terminus of Aβ42, is more active in patients with LOAD, suggesting that increased amyloid production processing might also contribute to the sporadic disease. Using high-throughput siRNA screening technology, we assessed 15,200 genes for their role in Aβ42 secretion and identified leucine-rich repeat transmembrane 3 (*LRRTM3*) as a neuronal gene that promotes APP processing by BACE1. siRNAs targeting *LRRTM3* inhibit the secretion of Aβ40, Aβ42, and sAPPβ, the N-terminal APP fragment produced by BACE1 cleavage, from cultured cells and primary neurons by up to 60%, whereas overexpression increases Aβ secretion. LRRTM3 is expressed nearly exclusively in the nervous system, including regions affected during AD, such as the dentate gyrus. Furthermore, *LRRTM3* maps to a region of chromosome 10 linked to both LOAD and elevated plasma Aβ42, and is structurally similar to a family of neuronal receptors that includes the NOGO receptor, an inhibitor of neuronal regeneration and APP processing. Thus, *LRRTM3* is a functional and positional candidate gene for AD, and, given its receptor-like structure and restricted expression, a potential therapeutic target.

Aβ | siRNA | RNAi | Chromosome 10 | NogoR

Alzheimer's disease (AD) is the most common form of dementia and a debilitating neurodegenerative disease. In the majority of cases, the disease presents after age 65 because of largely unknown causes. However, in familial AD (FAD), the likely pathogenic trigger is release of amyloidogenic Aβ peptides from amyloid-precursor protein (APP), a transmembrane domain protein present in neuronal and other cells (1). Aβ, the primary constituent of amyloid plaques, is generated from APP by proteolysis of the extracellular domain by BACE1 (Fig. 1*A*, 2), followed by intramembranous cleavage within its residual transmembrane domain by γ-secretase [composed of presenilin-1 (PSEN1) or -2 (PSEN2) plus nicastrin (NCSTN), aph-1 (APH1), and pen-2 (PSENEN) (3)]. γ-Secretase cleaves at multiple sites and yields mostly the 40-aa Aβ40 peptide along with the more amyloidogenic 42-aa Aβ42 (1). Alternatively, APP is cleaved by α-secretase within Aβ, resulting in nonamyloidogenic metabolites. Mutations in APP or the presenilins account for most cases of FAD, and all increase Aβ42 production from APP (1, 4, 5). These data are the basis of the amyloid hypothesis of AD.

In late-onset (LO)AD, the etiology is not understood, but the major genetic risk factor is *APOEε4*, which promotes Aβ deposition in the brains of mice (6), and BACE1 protein and activity are increased in LOAD (7–9). Furthermore, LOAD (10–12) and circulating Aβ42 (13) levels were independently linked to chromosome 10q21–22, suggesting that genetic modifiers of LOAD risk also regulate Aβ metabolism. These data raise the possibility that genes regulating Aβ metabolism will influence AD risk of sporadic disease.

Because siRNAs selectively inhibit the expression of a single target gene, siRNA screening technology allows for the parallel interrogation of thousands of genes for their role in a biological process. Thus, we developed a genome-scale approach to identify genes regulating the secretion of Aβ. We report here that LRRTM3 is a neuronal activator of BACE1 localized to the region of chromosome 10 associated with LOAD and plasma Aβ42 levels.

Results

An siRNA Screen for Genes Regulating Aβ42 Secretion. We generated HEK293T cells stably expressing APP containing N-terminal epitope tags and a substitution of 4 aa at the BACE1 cleavage site (NFEV for KMDA), which enhances BACE1 cleavage (14). These modifications permit miniaturized assays for the N-terminal products secreted by α- and β-secretase [sAPPα and sAPPβ_{NF} (NF or EV subscripts indicate the use of the NFEV substitution)] and both A$\beta40_{EV}$ and A$\beta42_{EV}$ (Fig. 1*A*). We assayed 15,200 siRNA pools, each consisting of three different siRNAs targeting the same gene, for effects on A$\beta40_{EV}$, A$\beta42_{EV}$, and cell viability (Fig. 1*B*). After applying selection criteria designed to maximize detection of siRNA pools that altered Aβ secretion while minimizing false positives due to cytotoxicity (Fig. 1*B*), we selected 1,623 siRNA pools for confirmation.

We evaluated these 1,623 siRNA pools in three independent experiments by measuring secretion of A$\beta40_{EV}$, A$\beta42_{EV}$, sAPPβ_{NF}, and sAPPα. The positive controls performed as expected (Fig. 7 *A–D*, which is published as supporting infor-

Author contributions: J.M. and W.J.R. contributed equally to this work; J.M., A.E., A.B.S., X.-P.S., D.B., and D.J.S. designed research; J.M., C.W., S.M., E.S., A.G., M.X., Q.H., L.M., K.G., P.S., J.B., D.C., B.P., and T.R. performed research; M.F., B.S., J.K., and A.S. contributed new reagents/analytic tools; S.B., M.S., D.H., K.S.K., G.R.S., and D.J.S. analyzed data; and W.J.R., J.M., and D.J.S. wrote the paper.

Conflict of interest statement: All authors are employed by Merck & Co., Inc. Rosetta Inpharmatics LLC is a wholly owned subsidiary of Merck & Co., Inc..

This article is a PNAS direct submission.

Freely available online through the PNAS open access option.

Abbreviations: AD, Alzheimer's disease; APP, β-amyloid precursor protein; CTF, C-terminal fragment; FAD, familial AD; LOAD, late-onset AD; LRR, leucine-rich repeat.

**To whom correspondence should be addressed at: Merck & Co., Inc., 770 Sumneytown Pike, West Point, PA 19486. E-mail: david_stone4@merck.com.

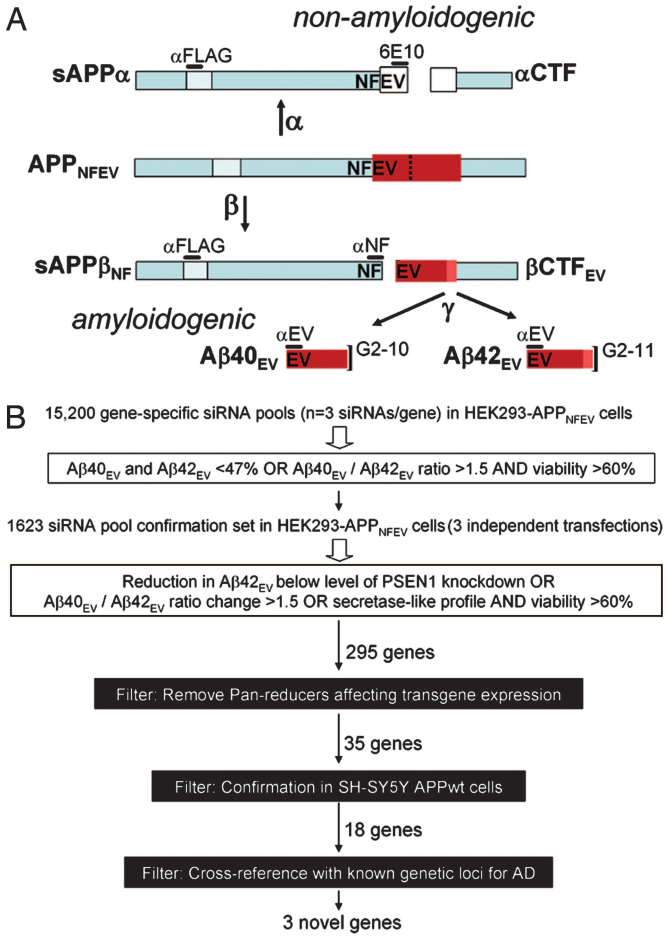

Fig. 1. An siRNA screen for APP processing. (*A*) APP processing by either α-secretase (nonamyloidogenic), generating sAPPα and the αCTF, or by BACE1 (amyloidogenic), generating sAPPβ$_{NF}$. The βCTF$_{EV}$ is a substrate for γ-secretase, producing the peptides Aβ40$_{EV}$ or Aβ42$_{EV}$. Antibodies used are shown. (*B*) Flow chart for siRNA screening and selection.

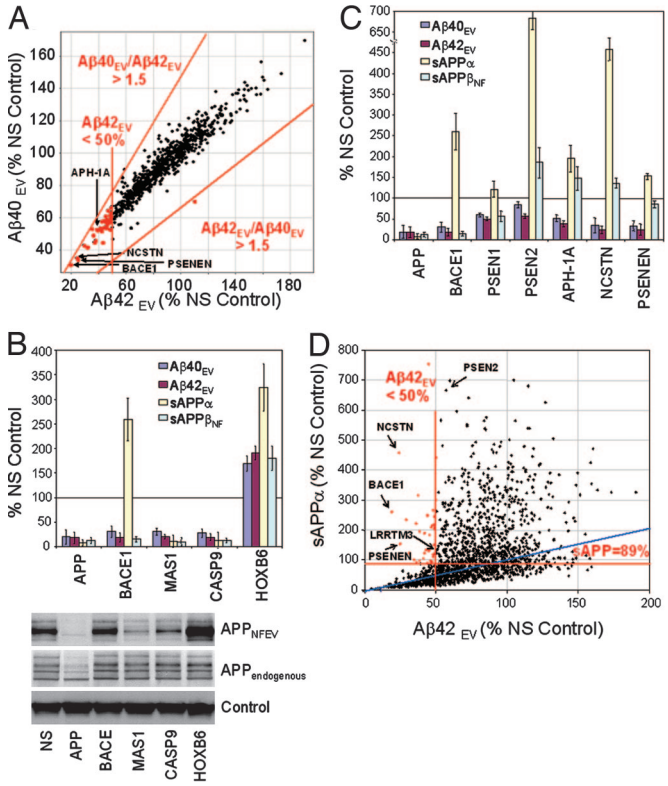

Fig. 2. Confirmation of primary screen data. (*A*) Shown is a scatter plot comparing the mean ($n = 3$) values of Aβ40$_{EV}$ to Aβ42$_{EV}$ for the 1,623 siRNA pools. siRNA pools lowering Aβ42$_{EV}$ values to 50% of control (vertical line) or altering the Aβ40$_{EV}$ to Aβ42$_{EV}$ ratio >1.5-fold are indicated in red. (*B*) Shown is the effect of example siRNAs that affect all four APP metabolites on APP transgene expression in HEK293 cells. (*Upper*) Mean ($n = 3$) effect of MAS1, CASP9, and HOXB6 siRNA pools on APP metabolite secretion. (*Lower*) 6E10 anti-APP Western blot for exogenous APP in HEK293 cells cotransfected with siRNAs and APP expression plasmid (*Top*) or endogenous APP in cells transfected with siRNA plus empty vector (*Middle*). βIII-tubulin served as control (*Bottom*). (*C*) Mean values for APP and secretase-targeting siRNAs normalized to nonsilencing controls derived from the secondary screen in HEK293 APP$_{NFEV}$ cells, showing that all lower Aβ without lowering sAPPα. (*D*) Scatter plot showing mean ($n = 3$) sAPPα versus Aβ42$_{EV}$ for siRNAs in the secondary screen of HEK293 APP$_{NFEV}$ cells. Secretase-like siRNAs raising sAPPα while lowering Aβ42$_{EV}$ are in the upper left quadrant. Error bars represent standard deviation.

mation on the PNAS web site). Because FAD mutations often alter the Aβ42$_{EV}$/Aβ40$_{EV}$ ratio (1), we first searched for siRNAs with that property (Fig. 2*A*). Only two yielded a ratio of 1.5 for Aβ40$_{EV}$/Aβ42 $_{EV}$ (EPB41 and WDR60), and one targeting PCDH11X (15) produced a ratio of 1.7 for Aβ42 $_{EV}$/Aβ40$_{EV}$.

Next, we examined siRNAs that affected both Aβ40$_{EV}$ and Aβ42$_{EV}$. Many of these siRNAs reduced all four metabolites, suggesting interference with APP transgene expression. To eliminate false positives, siRNAs that inhibited alkaline phosphatase expressed from the same plasmid backbone as APP >40% were eliminated. Remaining siRNAs were then analyzed for their effect on the *APP* transgene (Fig. 2*B*). CASP9, MAS1, and HOXB6 siRNAs had no effect on endogenous APP but strongly influenced plasmid-encoded APP. These and similar experiments indicate that most of the siRNAs lowering all four APP metabolites produced nonspecific effects through transgene repression.

Because siRNAs targeting BACE1 and γ-secretase components lower Aβ without lowering sAPPα, (Fig. 2*C*), comparisons of sAPPα and Aβ42$_{EV}$ levels identifies siRNAs that may inhibit Aβ secretion without repressing the transgene (Fig. 2*D*, upper left quadrant). This secretase-like profile (decreased Aβ and sAPPα not decreased) defined potential genetic modulators of APP processing. To test these criteria, we analyzed secretase-like siRNAs by using Gene Ontology (Table 1). The most significant enrichment of gene-associated terms was for β-amyloid metabolism ($P = 2.84 \times 10^{-14}$), confirming detection of APP regulators. Interestingly RNA splicing and the microtubule cytoskeleton were also implicated by this analysis.

Table 1. Gene Ontology results showing enrichment of terms assigned to the secretase-like siRNA hits for biological process and cellular component

GO gene set	Gene set size	Overlap	*P*
Biological process (input, 32 genes)			
β-amyloid metabolism	17	6	2.84×10^{-14}
RNA splicing	285	7	5.22×10^{-8}
Cell-fate commitment	55	3	1.91×10^{-5}
Cellular component (input, 25 genes)			
Spliceosome complex	92	5	2.69×10^{-8}
Microtubule cytoskeleton	348	5	1.91×10^{-5}

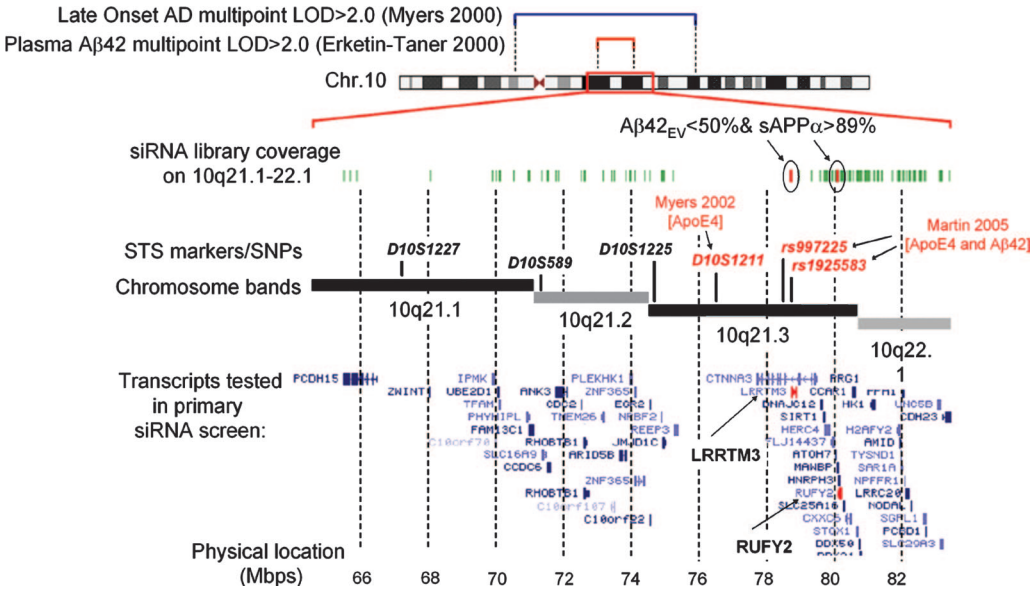

Fig. 3. Two siRNA hits mapped in close proximity to a genomic region associated with LOAD. Diagram of the genomic location of association studies for LOAD [blue bar; (26)] and plasma Aβ42 [red bar; (13)] superimposed over a map of chromosome 10. LOD, logarithm of odds for association. Shown below (*Upper*) are the locations of siRNAs in the library mapped to the region of overlap between the studies. STS markers and SNPs indicate the location of markers associated with LOAD or plasma Aβ42 in relation to chromosome bands and physical location in millions of base pairs (Mbps; National Center for Biotechnology Information). Red text indicates association with LOAD in *APOE ε4*-positive individuals in studies of *CTNNA3*: Genomic markers rs12357560 and rs7070570 have shown association ($P < 0.001$) with plasma Aβ42 in LOAD families (16). In *APOE ε4*, carriers rs997225 and rs1925583 have association values $P < 0.05$ in case-control population analysis of LOAD (27) Shown below (*Lower*) is a transcript density map showing the exon structure of selected genes. *LRRTM3* and *RUFY2* are indicated. Note the localization of *LRRTM3* within an intron of *CTNNA3*.

***LRRTM3* and *RUFY2* Map to Chromosome 10q21.** Secretase-like siRNAs were then mapped to genomic regions associated with LOAD. Two genes, *LRRTM3* and *RUFY2* reduce Aβ secretion (Fig. 4*A*) and map to chromosome 10q21, a location of overlap between independent studies of LOAD and circulating Aβ42 levels (10, 13) (Fig. 3). Interestingly *LRRTM3* resides within the large intron of the α-T catenin gene (*CTNNA3*), a positional candidate gene for LOAD (16). Genetic variability in the region upstream of *LRRTM3* has been associated with LOAD in APOE ε4-positive individuals (Fig. 3), and neither CTNNA3 siRNAs nor siRNAs targeting nearby genes produce a secretase-like effect in HEK293T or SH-SY5Y cells (Fig. 3*B*; and see Fig 8, which is published as supporting information on the PNAS web site). To validate the LRRTM3 siRNA pool, the three individual siRNA pool components, each targeting a different sequence, were tested, and all reduce Aβ40 dose-dependently (Fig. 4*C*). LRRTM3 siRNA pools reduce LRRTM3 RNA 5-fold but not APP, BACE1, or γ-secretase-component RNAs or the expression of APP protein (Fig. 4*D*). *LRRTM3* is predicted to encode a Type I receptor-like molecule possessing a series of leucine-rich repeat (LRR)-binding motifs in its putative extracellular domain, and thus shares homology with LRR-containing proteins such as slit1 and the Nogo receptor (RTN4R) (17) (Fig. 4*E*). Based on the above data, we selected *LRRTM3* for additional studies.

Role of LRRTM3 in APP Processing. To further characterize LRRTM3, we transfected siRNAs into SH-SY5Y human neuroblastoma cells (Fig. 9, which is published as supporting information on the PNAS web site). We first asked whether the other three LRRTM family member genes regulate APP processing. LRRTM3 siRNA reduces Aβ secretion (Fig. 5*A*), whereas siRNAs targeting LRRTM1 elevate $A\beta42_{EV}$. siRNAs against LRRTM4 and RTN4R siRNAs were not significant in these cells (RTN4R protein was not detected). Conversely transfection of LRRTM3-FLAG cDNA led to expression of an ≈68-kDa protein detectable by FLAG antibodies and enhanced secretion of Aβ, as did RTN4R cDNA (Fig. 5*B*). Examination of the intracellular C-terminal fragments (CTFs) produced by β-secretase and α-secretase (βCTF and αCTF) demonstrate that LRRTM3 siRNAs reduce βCTF. In contrast, LRRTM3 siRNAs do not cause γ-secretase substrates βCTF and αCTF to accumulate in cells overexpressing βCTF, whereas siRNAs targeting the γ-secretase subunits do (Fig. 5*C*). Thus, LRRTM3 modulates BACE1 processing of APP. To determine whether LRRTM3 acts directly on BACE1, LRRTM3 and BACE1 siRNAs were transfected into SH-SY5Y cells, and membrane preparations were assayed for BACE1 activity. LRRTM3 siRNAs do not significantly lower total BACE1 activity (Fig. 5*F*).

Expression and Activity of *LRRTM3*. Because most Aβ is generated in neurons (18), we examined the expression of *LRRTM3* in the brain. LRRTM3 mRNA is expressed nearly exclusively in the CNS (Fig. 6*A*; and see Fig. 10, which is published as supporting information on the PNAS web site) as reported (19). RT-PCR analysis of mouse brain indicates that LRRTM3 is expressed broadly by embryonic day 15 and accumulates thereafter (Fig. 6*B*). *In situ* hybridization studies show regional expression of LRRTM3, with high levels in cortical laminae and dentate gyrus, as well as detectable levels in the hypothalamus and amygdala (Fig. 6*C*).

LRRTM3 or control siRNAs were then cotransfected with eGFP and wild-type APP in cells isolated from the cortex and hippocampus of postnatal mice. After 5 days, LRRTM3 inhibition had no overt effect on survival (Fig. 6*D*) but reduced Aβ40 secretion 40%, an effect similar to BACE1 siRNAs. We then tested for colocalization of APP with LRRTM3. LRRTM3-FLAG cDNA was transfected along with APP into SH-SY5Y cells and visualized by FLAG immunofluorescence (IF). LRRTM3-FLAG immunoreactivity was detected in a punctate, vesicle-associated pattern consistent with its putative transmembrane localization (Fig. 6*F*). When APP IF images are merged with LRRTM3-FLAG images,

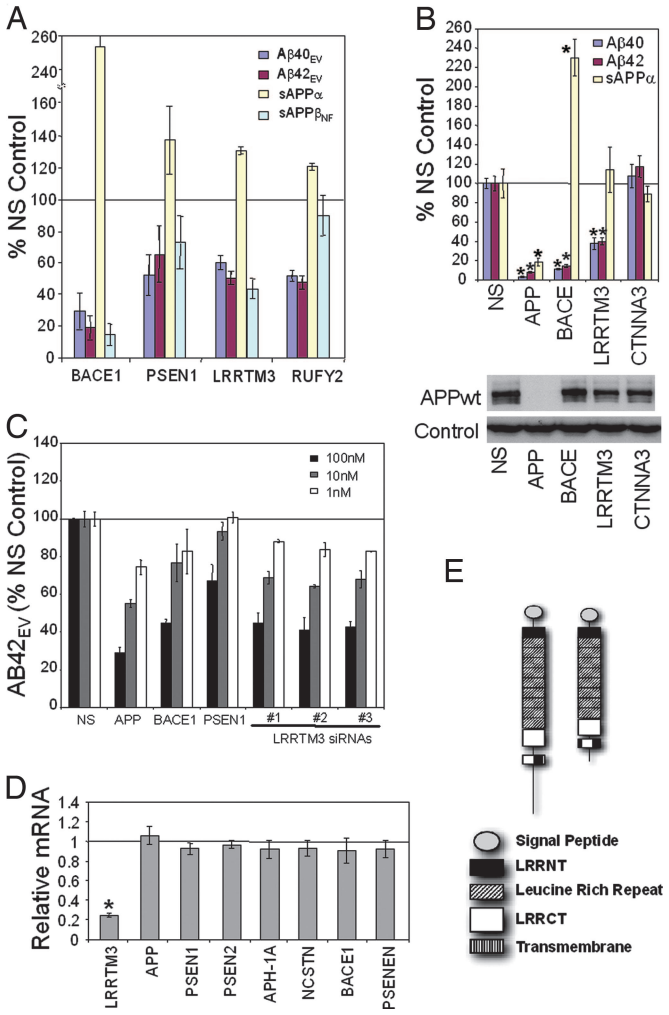

Fig. 4. LRRTM3 siRNA effects on APP processing. (*A*) Effect of LRRTM3 and RUFY2 on APP_{NFEV} secretion from HEK293 cells. Shown are mean ($n = 3$) values normalized to nonsilencing controls. (*B*) Mean ($n = 3$) effect of CTNNA3 and LRRTM3 siRNAs on wild-type APP processing in SH-SY5Y cells normalized to nonsilencing controls (*Upper*). (*B Lower*) APP Western blot of transfected cell lysates is shown (control is β-actin). (*C*) Mean ($n = 2$) normalized values for $A\beta40_{EV}$ secreted from HEK293 cells transfected with APP_{NFEV} and the indicated siRNAs at three doses; each LRRTM3 siRNA is a distinct component of the siRNA pool. (*D*) Branched DNA measurement of mRNA levels in SH-SY5Y cells after LRRTM3 siRNA transfection. Mean values for each indicated mRNA subtracted from GAPDH mRNA (internal control) and normalized to nonsilencing siRNA values (set to 1). (*E*) LRRTM3 and Nogo Receptor (RTN4R) domain structure predicted by CD-Search (National Center for Biotechnology Information). NT, amino terminal; CT, carboxy terminal domains. *, $P < 0.05$ by using ANOVA. Error bars indicate the standard deviation.

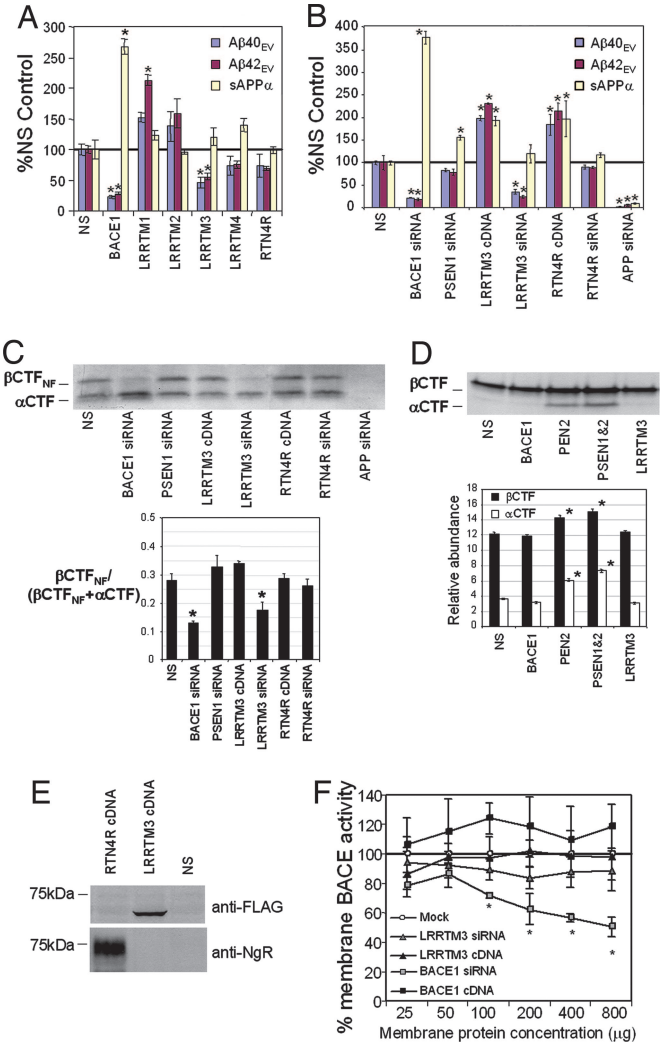

Fig. 5. LRRTM3 affects β-secretase processing of APP. (*A*) Effect of LRR family members on APP processing. siRNA pools targeting LRRTM1–4 and RTN4R were transfected into SH-SY5Y cells along with APP_{NFEV}. Unless noted, all values are means ($n = 3$) normalized to controls from separate experiments. (*B*) Effect of LRRTM3 overexpression on APP processing in SH-SY5Y cells. (*C Upper*) Western blot for the CTFs of APP_{NFEV} secretion (βCTF_{NF} and αCTF) and quantification of data from three experiments expressed as a ratio of βCTF_{NF} to total CTF (*Lower*). (*D*) Lack of effect on γ-secretase. The C-terminal 99 aa of APP, which correspond to the βCTF generated by BACE1, were expressed in SH-SY5Y cells cotransfected with siRNAs, as indicated. βCTF and αCTF were analyzed by Western blot (*Upper*), and mean ($n = 2$) optical densities are shown (*Lower*). (*E*) Western blot for LRRTM3-FLAG and RTN4R protein in transfected SH-SY5Y cells. (*F*) Membrane-associated BACE activity measurements from SH-SY5Y membranes from transfected cells at varying levels of membrane, as measured by micrograms of protein. Cleavage of a peptide substrate for BACE1 was measured at each dilution, and activity in the mock transfected membranes was set to 100%. At higher membrane concentrations, BACE1 activity was detectable, and siRNAs inhibited BACE1 activity, whereas LRRTM3 siRNA was not significant. *, $P < 0.05$, ANOVA. Error bars show the standard deviation.

LRRTM3-FLAG immunoreactivity is enriched in processes extending from the cells, many of which have little APP immunoreactivity, and extensive colocalization was not observed.

Discussion

Genetic studies of FAD have led to the amyloid hypothesis, which holds that imbalances in the metabolism of Aβ lead to neurodegeneration. An important question is whether the concepts developed from FAD apply to LOAD, because LOAD afflicts significantly more people. The effect of APOE on Aβ metabolism in the brains of transgenic mice (6), the overlap of genetic determinants of risk for LOAD and plasma Aβ42 on chromosome 10q21, and the elevated BACE1 protein and activity in AD (7–9) all suggest that altered Aβ metabolism contributes to LOAD pathogenesis.

We therefore screened 15,200 genes to identify regulators of APP processing. A large number of siRNAs scored positive, but as many as 90% were potentially affecting APP expression by interfering with the transgene (Fig. 2*B*). It remains to be determined whether any of these siRNAs regulate endogenous APP expression in the brain, because increased APP expression

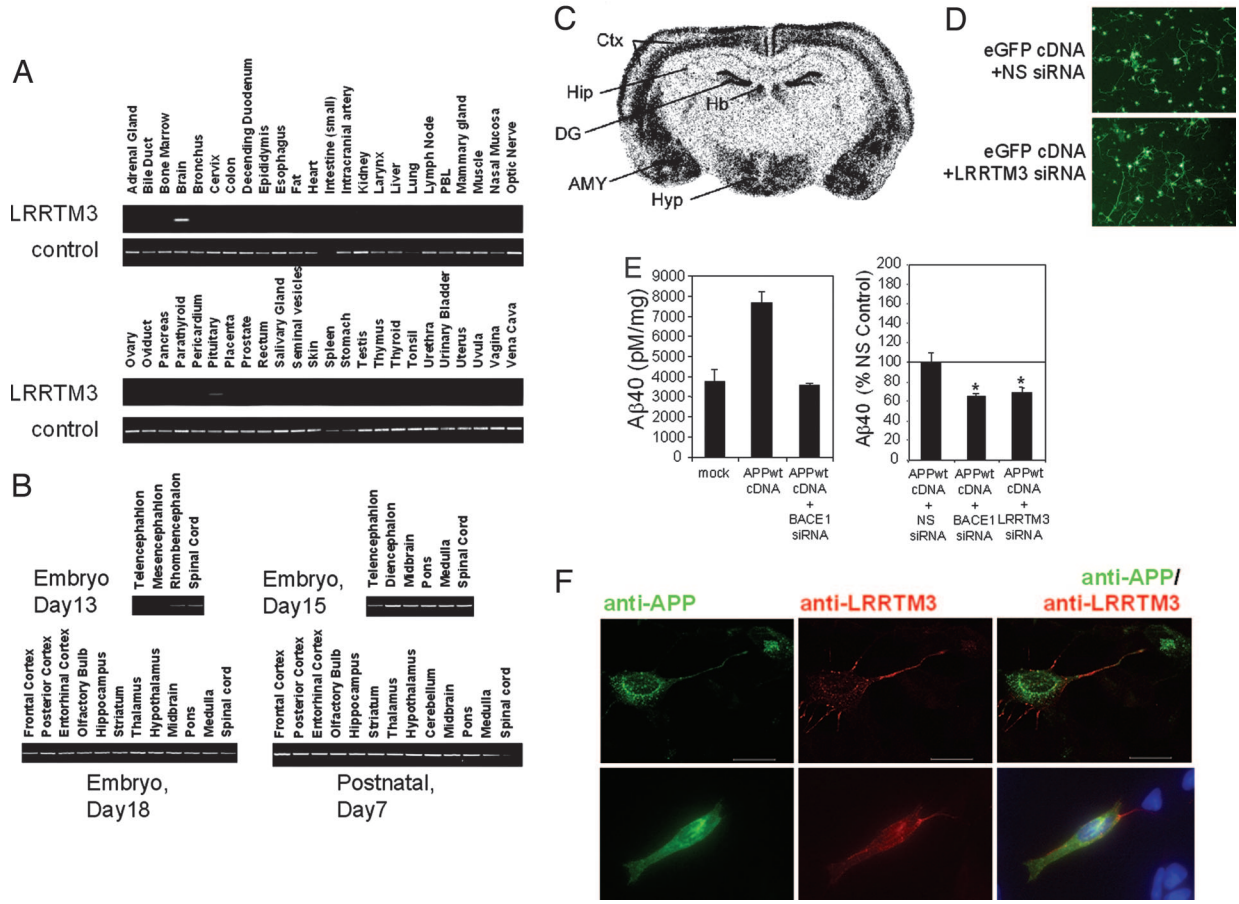

Fig. 6. Neuronal expression and activity of LRRTM3. (*A* and *B*) Semiquantitative PCR of cDNAs from 48 human tissues with gene-specific primers for *LRRTM3* (*A*) or mouse brain regions (*B*). (*C*) *In situ* hybridization with antisense probes to LRRTM3 in adult mouse brain (coronal section with standard anatomical markers). Ctx, cortex; Hip, hippocampus; DG, dentate gyrus; AMY, amygdala; Hyp, hypothalamus; Hb, habenular. (*D*) Mouse cortical primary neurons at day 5, transfected with eGFP and indicated siRNA to illustrate transfection efficiency and allow visualization of morphology. (*E Left*) Mean Aβ40 from conditioned medium of mouse primary neurons transfected with wild-type APP ± BACE1 siRNAs. (*E Right*) Mean Aβ40 levels normalized to nonsilencing (NS) controls for primary neurons cotransfected with cDNA encoding wild-type APP plus BACE1 or LRRTM3 siRNAs. (*F*) Standard (*Lower*) and confocal (*Upper*) immunofluorescence images of SH-SY5Y cells cotransfected with APP and LRRTM3-FLAG cDNAs. The right image is merged. *, $P < 0.05$ ANOVA. Error bars represent the standard deviation. (Scale bar, 20 μM.)

may influence risk of LOAD (20). No siRNA pool dramatically altered the site-selectivity of γ-secretase, whereas many affected both Aβ40 and Aβ42 similarly. This lack of differential regulation argues against models in which the two species of Aβ are generated independently.

We identified two regulators of APP processing mapping to the region of chromosome 10 associated with LOAD and plasma Aβ42, *LRRTM3* and *RUFY2*. We focused on *LRRTM3* because of its proximity to genetic variability associated with LOAD in *APOE ε4*-positive individuals (Fig. 3), its similarity to the Nogo receptor (Fig. 4*E*), its neuronal expression pattern (Fig. 6), and its effect on BACE1 (Fig. 5). Although the mechanism by which LRRTM3 influences BACE1 processing of APP is unknown, our data suggests that LRRTM3 might act through vesicle trafficking or signaling, because LRRTM3 siRNAs do not significantly inhibit total BACE activity, the transcription of secretases (Figs. 4*D* and 5*F*), or APP expression and maturation (Fig. 4*B*). Furthermore, LRRTM3-FLAG protein does not extensively colocalize with APP in SH-SY5Y cells but, instead, distributes toward the periphery, particularly in long processes (Fig. 6*F*). It remains possible that LRRTM3 mediates BACE1 activity or substrate presentation in discreet subcellular locations.

Within the mouse hippocampus, LRRTM3 is restricted to the dentate gyrus, a critical structure in AD pathology (21). The dentate gyrus receives cortical input to the hippocampus from the entorhinal cortex via the perforant pathway. Lesions of this pathway impair memory, which is notable, given that early-stage AD shows substantial loss of entorhinal cortex neurons (22) and that Tg2576 transgenic mice lose spine density in the dentate gyrus a year before plaque formation (23). Furthermore, in transgenic mice, lesions of the perforant pathway reduce amyloid burden in the dentate gyrus by 45% (24). Thus, LRRTM3 is expressed within a structure important for both memory and amyloid production.

In summary, these findings demonstrate the utility of functional genomics for identifying genes potentially involved in AD. Furthermore, the receptor-like structure of LRRTM3 combined with its CNS-restricted expression suggests that it could be a therapeutic target.

Materials and Methods

Cell Lines and Reagents. HEK293T/APP_{NFEV} cells stably express APP_{NFEV}, which encodes human APP, isoform 1–695 with HA, Myc, and FLAG inserted at position 289 and NFEV for KMDA at 595–598 (14). Anti-NF and anti-EV antibodies were affinity purified to detect the C terminus of $sAPP\beta_{NF}$ and the N terminus of the Aβ peptides, respectively. Bio-G210 and Bio-G211 antibodies (Genetics Company, Zurich, Switzerland) were used to

detect the C termini of $A\beta 40_{EV}$ and $A\beta 42_{EV}$, respectively. 6E10 antibody (Signet Laboratories, Dedham, MA) was used to capture $A\beta 40_{EV}$ and $A\beta 42_{EV}$ peptides, whereas Bio-M2 anti-Flag (Sigma, St. Louis, MO) was used to capture N-terminal secreted products. Details are in *Supporting Methods*, which is published as supporting information on the PNAS web site.

siRNA Library. The custom siRNA library (synthesized by Sigma–Proligo) was composed of 45,600 siRNAs targeting 15,200 unique genes with three siRNAs per gene. All siRNAs passed both vendor and internal quality control. siRNAs were designed by an algorithm that increases efficiency of the siRNAs while minimizing off-target effects (16). The siRNAs have sequence asymmetry and have undergone sequence alignment to eliminate siRNAs with at least 17 bp of complementarity to other genes, repeat masking, masking of the 5′ untranslated region, and restrictions on nucleotide number to allow for design in the 3′ untranslated region. For genes with multiple splice forms, the common sequence was targeted.

siRNA Data Analysis. By analyzing the 300 replicates of control siRNAs in the primary screen, a cutoff of $A\beta 42 < 47\%$ of control had 90% power to detect BACE1, 75% power to detect NCSTN, and 80% power to detect PSENEN while detecting the NS control as a false positive <1%. siRNAs selected for confirmation were required to have a viability of at least 60% as well as to fall into one of the following categories: $A\beta 42_{EV}$ level <47% or $A\beta 42_{EV}$ level >150%; $40/42 > 1.5$ or $42/40 > 1.5$. In the secondary screen, siRNAs were classified as "secretase-like" based on mean reductions of $A\beta 40_{EV}$ and $A\beta 42_{EV}$ >2 SD (as measured with nonsilencing siRNA, 1 SD = 8.5% and 11.5%, respectively) with sAPPα >89%, (one standard error below mean for controls). Gene Ontology analysis is described in *Supporting Methods*.

siRNA Transfection, Aβ ELISA, and Western Blot. In HEK293 cells, the transfection procedure above was scaled for 96-well plates without γ-secretase inhibitor. For transfection of SH-SY5Y cells, 2×10^6 cells were transfected with cDNAs and siRNAs by using a nucleofector system and program A-023 as recommended by manufacturer (Amaxa, Gaithersburg, MD). After overnight incubation, fresh media were conditioned for 48 h. For ELISA, 50 μl of media plus 50 μl of alkaline phosphatase (AP)-conjugated G210 (for Aβ40 detection), 12F4 (for Aβ42 detection), or P2–1 (for sAPPα detection) was incubated on ELISA plates coated with 6E10 (Tables 2–5, which are published as supporting information on the PNAS web site). After overnight incubation and washing, AP substrate was added, and chemiluminescence was measured. APP holoprotein was analyzed by 4–20% SDS-PAGE with 30 μg of total protein, followed by 6E10 detection on nitrocellulose. siRNA sequences are provided in the *Supporting Methods*.

RNA Expression. The *in situ* hybridization method has been described (25). The autoradiograms were digitized (MCID M5;Imaging Research, St. Catherines, ON, Canada), processed for brightness/contrast enhancement, and imported into Photoshop (Adobe Software, Mountain View, CA) where anatomical landmarks were added. To measure relative mRNA expression, SH-SY5Y cells were treated with target or NS siRNA as above, and mRNAs levels were determined by using the Quantigene reagent system (Panomics, Fremont, CA). GAPDH, APP, BACE1, PSEN1 and -2, APH-1A, NCSTN, PSENEN, and LRRTM3 probe sets were obtained through Panomics and used to measure each message. mRNA expression is presented as a ratio of NS siRNA-treated control normalized to internal GAPDH. For semiquantitative PCR, cDNA was amplified with gene-specific primers for 34 cycles following manufacturer's recommendation (Open Biosystems, Huntsville, AL).

BACE Activity Assay. Details are provided in *Supporting Methods*. Briefly, resuspended membrane preparations from SH-SY5Y cells transfected with either siRNA or cDNA were serially diluted and incubated with 250 mM biotinylated BACE1 substrate for 24 h at 37°C. Product was detected with ruthenium labeled neoepitope antibody and streptavidin-labeled Dynabeads.

Immunofluorescence. SH-SY5Y cells transfected with APPwt and LRRTM3 containing a C-terminal FLAG epitope tag (LRRTM3-FLAG) were fixed 48 h after transfection cells with 4% paraformaldehyde, washed with TBS, and treated with 0.2% Triton X-100 and 10% goat serum. Primary antibodies (anti-FLAG and 6E10) were incubated overnight in 0.05% Triton X-100 and 2.5% goat serum at 4°C. LRRTM3-FLAG was visualized with anti-mouse Alexa Fluor 555 and APP with anti-rabbit Alexa Fluor 488. All wells received 1:1,000 DAPI.

1. Selkoe DJ, Podlisny MB (2002) *Annu Rev Genomics Hum Genet* 3:67–99.
2. Vassar R, Bennett BD, Babu-Khan S, Kahn S, Mendiaz EA, Denis P, Teplow DB, Ross S, Amarante P, Loeloff R, *et al.* (1999) *Science* 286:735–741.
3. Edbauer D, Winkler E, Regula JT, Pesold B, Steiner H, Haass C (2003) *Nat Cell Biol* 5:486–488.
4. Scheuner D, Eckman C, Jensen M, Song X, Citron M, Suzuki N, Bird TD, Hardy J, Hutton M, Kukull W, *et al.* (1996) *Nat Med* 2:864–870.
5. Younkin SG (1998) *J Physiol (Paris)* 92:289–292.
6. Bales KR, Dodart JC, DeMattos RB, Holtzman DM, Paul SM (2002) *Mol Interv* 2:363–375:339.
7. Fukumoto H, Cheung BS, Hyman BT, Irizarry MC (2002) *Arch Neurol* 59:1381–1389.
8. Holsinger RM, McLean CA, Beyreuther K, Masters CL, Evin G (2002) *Ann Neurol* 51:783–786.
9. Tyler SJ, Dawbarn D, Wilcock GK, Allen SJ (2002) *Biochem Biophys Res Commun* 299:373–376.
10. Myers A, Holmans P, Marshall H, Kwon J, Meyer D, Ramic D, Shears S, Booth J, DeVrieze FW, Crook R, *et al.* (2000) *Science* 290:2304–2305.
11. Grupe A, Li Y, Rowland C, Nowotny P, Hinrichs AL, Smemo S, Kauwe JS, Maxwell TJ, Cherny S, Doil L, *et al.* (2006) *Am J Hum Genet* 78:78–88.
12. Curtis D, North BV, Sham PC (2001) *Ann Hum Genet* 65:473–481.
13. Ertekin-Taner N, Graff-Radford N, Younkin LH, Eckman C, Baker M, Adamson J, Ronald J, Blangero J, Hutton M, Younkin SG (2000) *Science* 290:2303–2304.
14. Shi XP, Tugusheva K, Bruce JE, Lucka A, Chen-Dodson E, Hu B, Wu GX, Price E, Register RB, Lineberger J, *et al.* (2005) *J Alzheimers Dis* 7:139–148;discussion 173–80.
15. Yagi T, Takeichi M (2000) *Genes Dev* 14:1169–1180.
16. Ertekin-Taner N, Ronald J, Asahara H, Younkin L, Hella M, Jain S, Gnida E, Younkin S, Fadale D, Ohyagi Y, *et al.* (2003) *Hum Mol Genet* 12:3133–3143.
17. Chen Y, Aulia S, Li L, Tang BL (2006) *Brain Res Brain Res Rev* 51:265–274.
18. Rossner S, Apelt J, Schliebs R, Perez-Polo JR, Bigl V (2001) *J Neurosci Res* 64:437–446.
19. Lauren J, Airaksinen MS, Saarma M, Timmusk T (2003) *Genomics* 81:411–421.
20. Theuns J, Brouwers N, Engelborghs S, Sleegers K, Bogaerts V, Corsmit E, De Pooter T, van Duijn CM, De Deyn PP, Van Broeckhoven C (2006) *Am J Hum Genet* 78:936–946.
21. Morrison JH, Hof PR (1997) *Science* 278:412–419.
22. Gomez-Isla T, Price JL, McKeel DW, Jr, Morris JC, Growdon JH, Hyman BT (1996) *J Neurosci* 16:4491–4500.
23. Jacobsen JS, Wu CC, Redwine JM, Comery TA, Arias R, Bowlby M, Martone R, Morrison JH, Pangalos MN, Reinhart PH, Bloom FE (2006) *Proc Natl Acad Sci USA* 103:5161–5166.
24. Sheng JG, Price DL, Koliatsos VE (2002) *J Neurosci* 22:9794–9799.
25. Ky B, Shughrue PJ (2002) *J Histochem Cytochem* 50:1031–1037.
26. Myers A, Wavrant De-Vrieze F, Holmans P, Hamshere M, Crook R, Compton D, Marshall H, Meyer D, Shears S, Booth J, *et al.* (2002) *Am J Med Genet* 114:235–244.
27. Martin ER, Bronson PG, Li YJ, Wall N, Chung RH, Schmechel DE, Small G, Xu PT, Bartlett J, Schnetz-Boutaud N, *et al.* (2005) *J Med Genet* 42:787–792.